

Figure 3. Part of Viking photomosaic of MTM-20272 quadrangle showing the intercrater plains (unit Npi), which are characterized by a smooth to irregular surface dissected by large-scale, well-incised valley networks and contain many impact craters exhibiting various degrees of preservation. In several places and at different scales, the main trunk valley of Vichada Valles splits and rejoins downstream (arrows). The image also shows a large crater (34 km diam) that is breached along its west rim by an inlet valley and along its southeast rim by an outlet valley. Most craters in the map area contain deposits of crater floor material (unit HNcf), presumably consisting of material eroded from the crater rim, deposited by eolian processes, or deposited via fluvial or lacustrine processes as in the case of crater 8. Locations of figures 4 and 5A-C are shown. North at top; image centered at lat 20° S, long 272.2° W; illumination from upper right. See figure 2 for figure location.

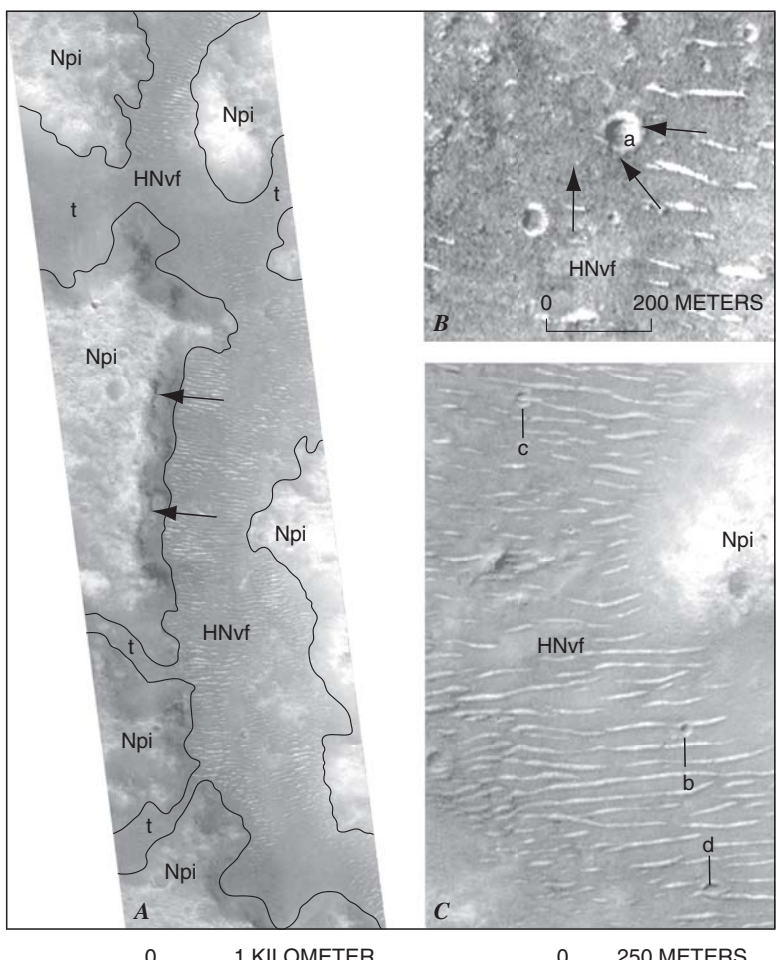


Figure 4. MOC image M04-00851 showing typical intercrater plains material (unit Npi). The plains display a surface pockmarked with many small (<1 km diam) degraded craters with morphologies ranging from visible rims and some infilling (white arrows) to little or no rim and almost completely filled interiors (red arrows). Most low-lying areas, such as craters, valleys (v, white arrow points downstream), and other depressions, are filled with dark sediments that generally form dunes, such as in crater 8. North at top; image centered at lat 21.4° S, long 272.1° W; image width, 2.88 km; resolution, 1.41 m/pixel; illumination from left; image from NASA/JPL/MSSS (available at http://www.msss.com/). See figures 2 and 5 for figure location.

Figure 5. MOC image M08-02977 (A) shows part of the trunk valley and some tributaries (t) of Vichada Valles within the intercrater plains (unit Npi). Layers or terraces are exposed along the east-facing wall of the trunk valley (arrows) indicating stratigraphy within the plains material and (or) evidence of flow events. Most valleys in the map area contain valley floor material (unit HNcf), which commonly consists of sediments remobilized to form parallel sets of dunes oriented orthogonal to valley walls (A-C). Crosscutting relations between impact craters and dunes are shown in B and C. In B, ejecta (arrows) from an ~80-m-diameter crater (8) superposes dunes and, in C, crater 8 appears to bisect a dune, whereas craters C and d are superposed by dunes. North is to the top in each image. M08-02977 (A): image centered at lat 20.7° S, long 272.8° W; image width, 2.88 km; resolution, 2.81 m/pixel. M04-02305 (B): image centered at lat 19.1° S, long 271.5° W; image width, 2.16 km; resolution, 2.62 m/pixel. M19-00428 (C): image centered at lat 19.2° S, long 272.1° W; image width, 1.44 km; resolution, 2.82 m/pixel. Illumination from left for A-C; images from NASA/JPL/MSSS (available at http://www.msss.com/). See figures 2 and 3 for figure location.

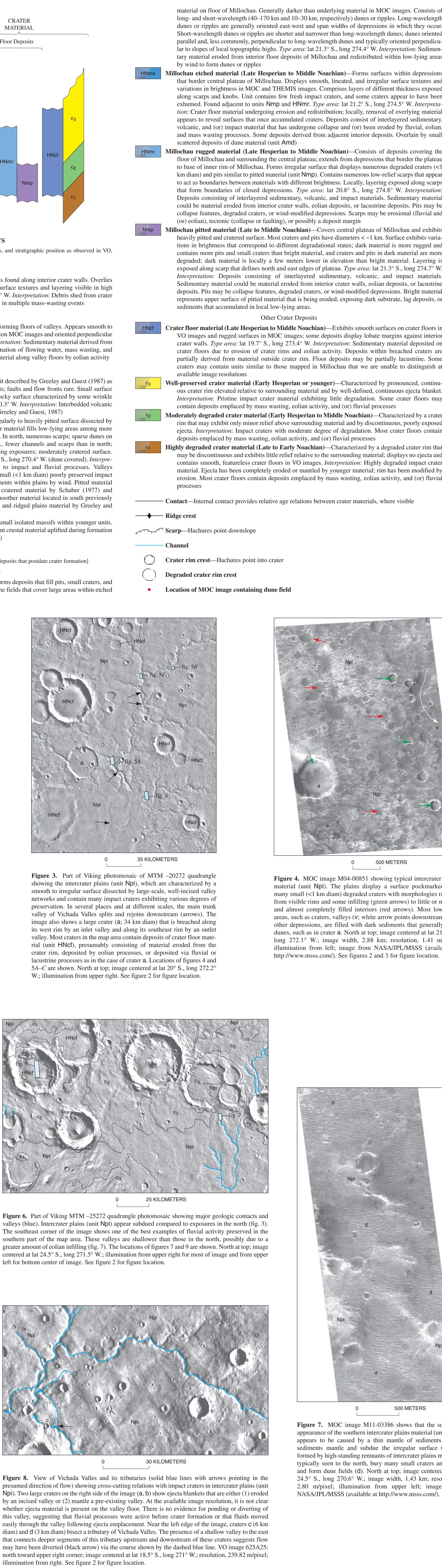


Figure 6. Part of Viking MTM-25272 quadrangle photomosaic showing major geologic contacts and valleys (blue). Intercrater plains (unit Npi) appear subdued compared to exposures in the north (fig. 3). The southeast corner of the image shows one of the best examples of fluvial activity preserved in the southern part of the map area. These valleys are shallower than those in the north, possibly due to a greater amount of eolian infilling (fig. 7). The locations of figures 7 and 9 are shown. North at top; image centered at lat 21.5° S, long 271.5° W; illumination from upper right for most of image and from upper left for bottom center of image. See figure 2 for figure location.

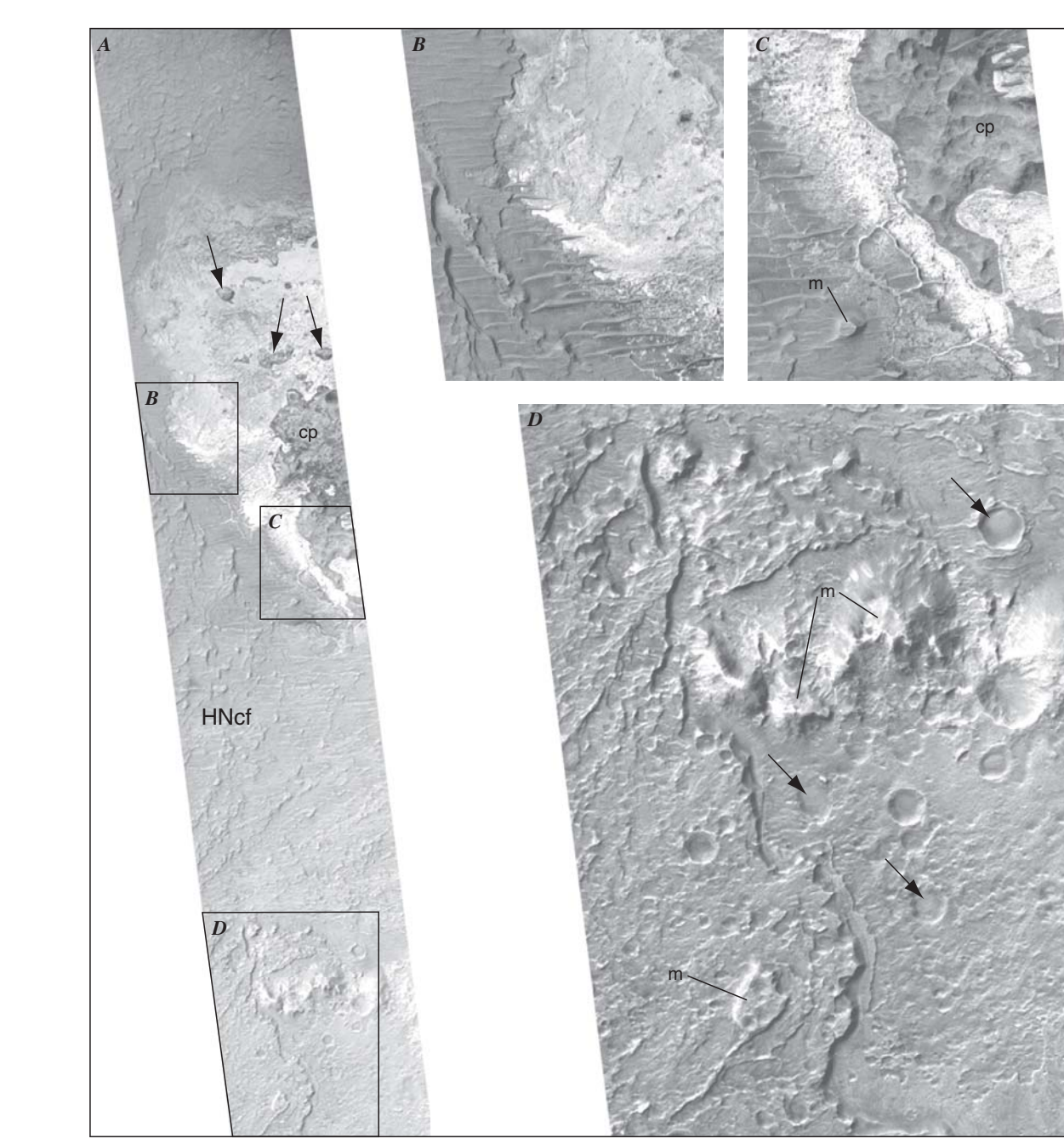


Figure 7. MOC image M11-03386 shows that the subdued appearance of the southern intercrater plains material (unit Npi) appears to be caused by a thin mantle of sediments. Dark sediments mantle and subdue the irregular surface textures that could be remnants of surfaces B or C. Surface D, separated by a data gap, contains mostly small degraded craters and appears the least eroded of the surfaces. Dune forms, visible in the close-up, are found in the low-lying areas of surfaces B and d, suggesting eroded sediments have been remobilized within this crater. North at top; image centered at lat 21.2° S, long 273.9° W; image width, 1.45 km; resolution, 2.83 m/pixel; illumination from left; image from NASA/JPL/MSSS (available at http://www.msss.com/). See figures 2 and 10 for figure location.

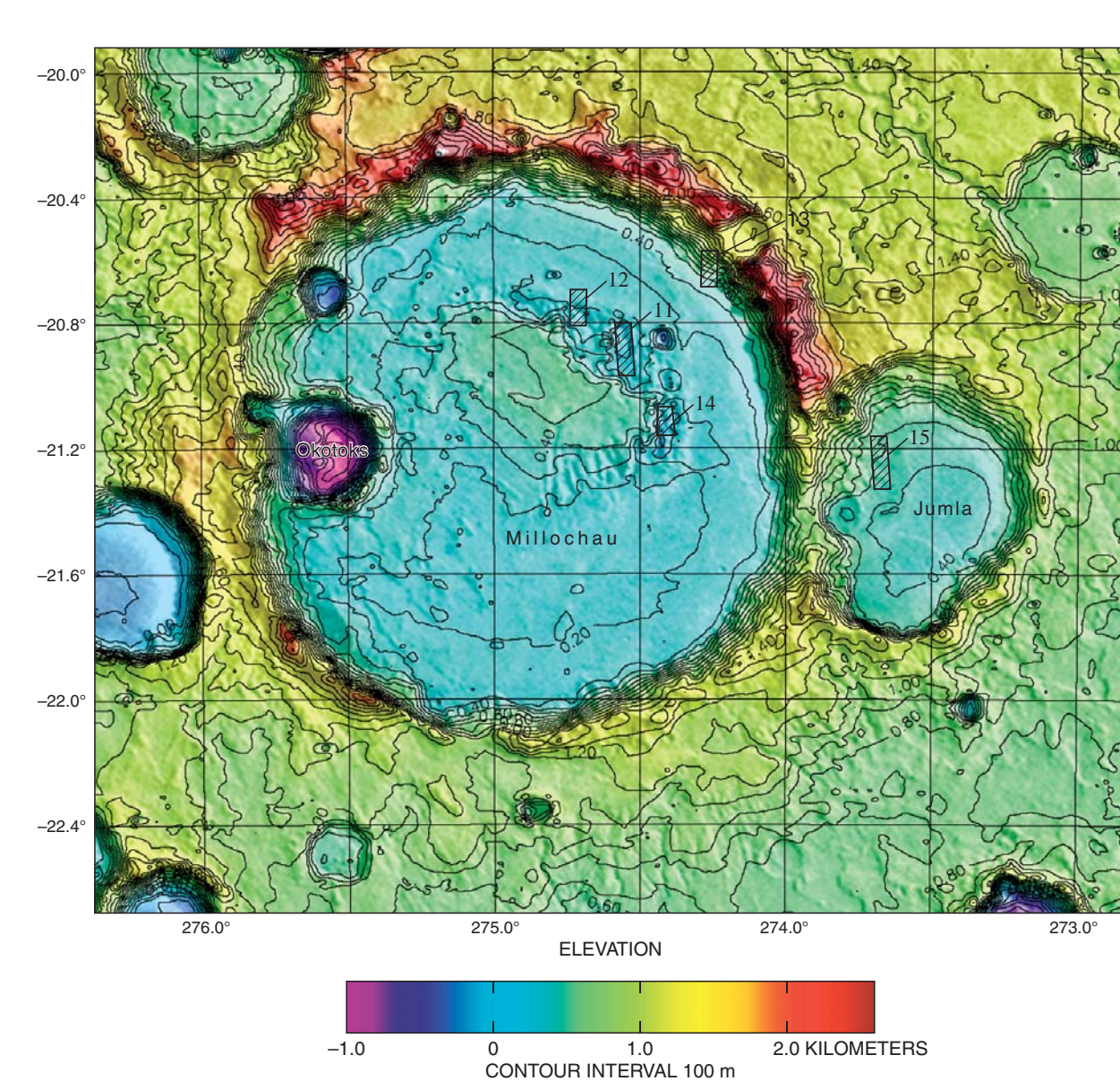


Figure 8. View of Vichada Valles and its tributaries (solid blue lines with arrows pointing in the presumed direction of flow) showing cross-cutting relations with impact craters in intercrater plains (unit Npi). Two large craters on the right side of the image (8, d) show ejecta blankets that are either (1) eroded by an incised valley or (2) mantle a pre-existing valley. At the available image resolution, it is not clear whether ejecta material is present on the valley floor. There is no evidence for ponding or diverting of this valley, suggesting that fluvial processes were active before crater formation or that fluids moved easily through the valley following ejecta emplacement. Near the left edge of the image, craters c (6 km diam) and d (3 km diam) bisect a tributary of Vichada Valles. The presence of a shallow valley to the east that connects deeper segments of this tributary upstream and downstream of these craters suggests flow may have been diverted (black arrow) via the course shown by the dashed blue line. VO image 62A425; north toward upper right corner; image centered at lat 18.5° S, long 271° W; resolution, 239.82 m/pixel; illumination from right. See figure 2 for figure location.

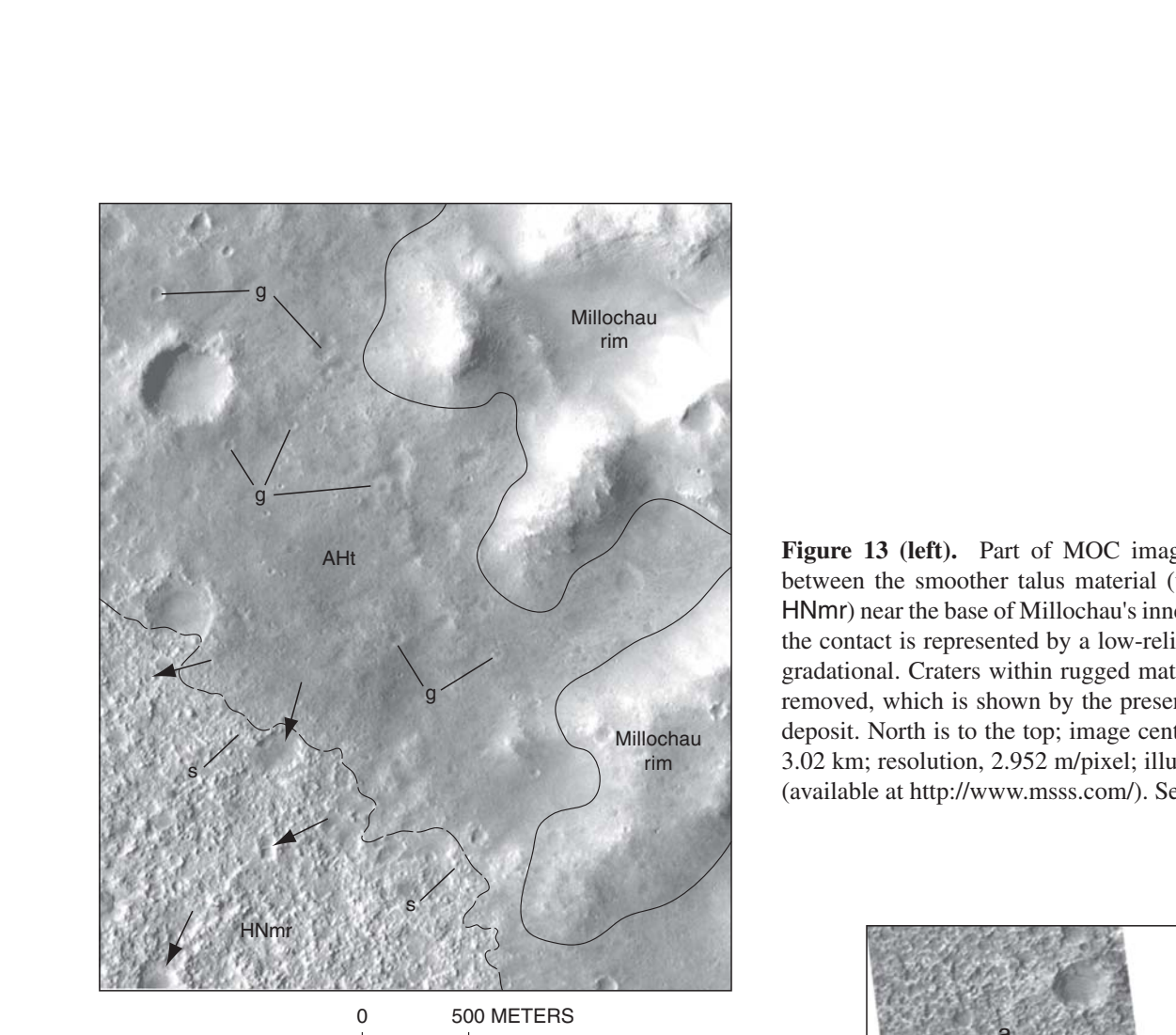


Figure 9. MOC image E16-01083 (A) showing crater floor material (unit HNcf) within a 36-km-diameter crater at lat 23.5° S, long 273.5° W. Crater floor material exhibits irregular surfaces and layering is visible in close-ups B-C. A rugged and cratered plateau (cp), located just northeast of this crater's center, is visible in C and is surrounded by very bright deposits (8, C) that appear to embay the plateau or were exposed upon erosion of the rugged surface. Possible outlines of the plateau are also visible in image A (arrows). Surrounding and apparently overlying the bright material are layered deposits that display irregular surfaces (B-D); some layers were eroded to form mesas (m; see C, D) and reveal exhumed craters (arrows in D). Dunes observed in B and C superpose the bright and layered material. Close-ups B-D are shown at the same scale. Image A centered at lat 23.9° S, long 273.3° W; image width, 3.03 km; resolution, 2.95 m/pixel; illumination from upper left; image from NASA/JPL/MSSS (available at http://www.msss.com/). See figures 2 and 10 for figure location.

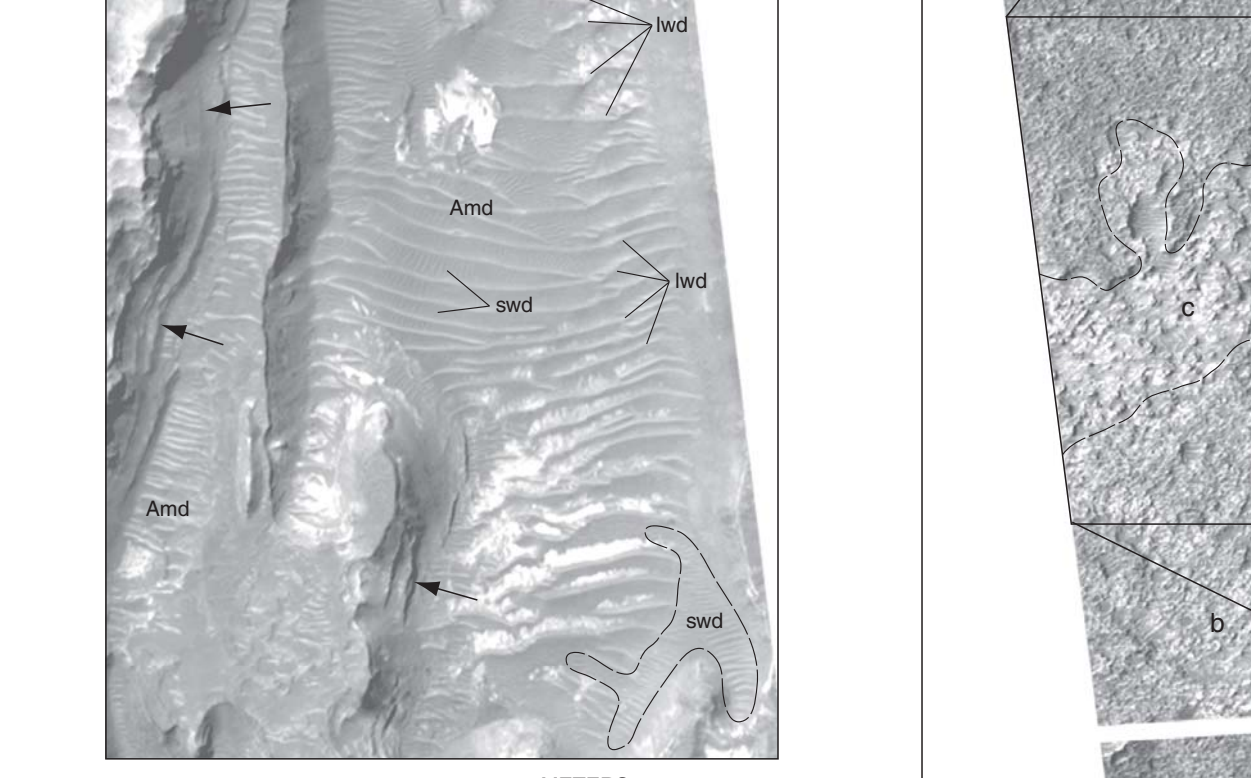


Figure 10. Millochau crater (114 km diam) and surrounding terrain shown as merged Viking MDM 2 and MOLA elevation data. The north and south rims of Millochau display striking differences in relief with the north rim being higher and steeper. Gullies along the south rim are evidence for enhanced erosion in this part of Millochau. Also note the raised plateau in the north-central part of Millochau, which is bounded on the north and east by large depressions. The locations of figures 11-15 are shown. North at top; figure centered at lat 21.1° S, long 274.5° W. See figure 2 for figure location.



Figure 11. Part of MOC image E01-01209 showing linedated (middle) and irregular (bottom) Millochau etched (unit HNme) and etched (unit HNmp) materials; a black line shows the contact between these units. Typical rugged material found within Millochau has a stucco-like texture and contains impact craters (c) that are heavily degraded. Etched material is irregular and contains several large knobs (k). Dune material (unit Arnd) fills low areas of the etched material. North at top; image centered at lat 20.7° S, long 274.7° W; image width, 2.8 km; resolution, 2.81 m/pixel; illumination from upper left; image from NASA/JPL/MSSS (available at http://www.msss.com/). See figures 2 and 10 for figure location.

Figure 12. Part of MOC image M19-01414 showing Millochau rugged unit (HNmr) and etched (unit HNmp) materials; a black line shows the contact between these units. Typical rugged material found within Millochau has a stucco-like texture and contains impact craters (c) that are heavily degraded. Etched material is irregular and contains several large knobs (k). Dune material (unit Arnd) fills low areas of the etched material. North at top; image centered at lat 20.7° S, long 274.7° W; image width, 2.8 km; resolution, 2.81 m/pixel; illumination from upper left; image from NASA/JPL/MSSS (available at http://www.msss.com/). See figures 2 and 10 for figure location.

Figure 13 (left). Part of MOC image R04-01308 showing the contact (dashed line) between the smoother talus material (unit AHt) and the irregular rugged material (unit HNmr) near the base of Millochau's inner wall (rim, right side of image). At some locations the contact is represented by a low-relief scarp (8), whereas in most places the contact is gradational. Craters within rugged material are being exhumed as talus material is being removed, which is shown by the presence of numerous ghost craters (g) within the talus deposit. North is to the top; image centered at lat 20.7° S, long 274.2° W; image width, 3.02 km; resolution, 2.952 m/pixel; illumination from left; image from NASA/JPL/MSSS (available at http://www.msss.com/). See figures 2 and 10 for figure location.

Figure 14. Part of MOC image M18-00592 showing both long- and short-wavelength dunes visible in one of the larger exposures of dune material (unit Arnd) in Millochau. Long-wavelength dunes (wd) are typically oriented east-west and span the widths of the depressions in which they occur. Short-wavelength dunes (swd) occur at all orientations, typically forming perpendicular to topographic highs, such as at the base of the layered knobs (arrows). Short-wavelength dunes also form perpendicular to the long-wavelength dunes as seen in the center of the image. North at top; image centered at lat 21.1° S, long 274.4° W; image width, 2.8 km; resolution, 2.81 m/pixel; illumination from left; image from NASA/JPL/MSSS (available at http://www.msss.com/). See figures 2 and 10 for figure location.

Figure 15. MOC image E04-02035 showing talus material (unit AHt) at the base of the inner rim of Jumbula, a 43-km-diameter crater that adjoins the east rim of Millochau. Talus material displays several surfaces (8-d) that appear to reflect different amounts of erosion. Surface 8 appears to be the uppermost layer in this sequence and displays distinct, yet degraded, crater forms. Surface b also displays degraded craters (see close-up), which are less distinct than those on surface 8. Surface c (see close-up) contains knobs and mesas that could be remnants of surfaces B or C. Surface d, separated by a data gap, contains mostly small degraded craters and appears the least eroded of the surfaces. Dune forms, visible in the close-up, are found in the low-lying areas of surfaces B and d, suggesting eroded sediments have been remobilized within this crater. North at top; image centered at lat 21.2° S, long 273.9° W; image width, 1.45 km; resolution, 2.83 m/pixel; illumination from left; image from NASA/JPL/MSSS (available at http://www.msss.com/). See figures 2 and 10 for figure location.

Geologic Map of MTM-20272 and -25272 Quadrangles, Tyrrhena Terra Region of Mars

By Scott C. Mest¹ and David A. Crown² 2006

¹NASA Goddard Space Flight Center, Planetary Geodynamics Laboratory, Greenbelt, MD 20771
²Planetary Science Institute, Tucson, AZ 85719